JOURNAL OF RESEARCH of the National Bureau of Standards—A. Physics and Chemistry
Vol. 77A, No. 6, November–December 1973

Nuclear Magnetic Resonance of ^{113}Cd and ^{199}Hg in Cd-Mg and Cd-Hg Solid Solutions

V. V. Zhukov,* I. D. Weisman, and L. H. Bennett

Institute for Materials Research, National Bureau of Standards, Washington, D.C. 20234

(August 10, 1973)

The current theoretical and experimental situation with respect to Knight shifts and bulk susceptibility of Cd in pure Cd and in Cd-Mg and Cd-Hg alloys is reviewed. New experimental isotropic and anisotropic Knight shift data on ^{113}Cd in Cd-Mg and Cd-Hg alloys and on ^{199}Hg in Cd-Hg alloys are presented. The behavior of the ^{199}Hg sites is found to be remarkably similar to that of the ^{113}Cd site in the Cd-Hg alloys. However the ratio of isotropic Knight Shift of ^{199}Hg to ^{113}Cd is somewhat greater than the ratio of ^{199}Hg to ^{113}Cd atomic hyperfine fields suggesting that there is more local electronic "*s*" character at the Fermi surface in the alloy than in the pure metals. This is consistent with the theoretical picture of Cd in which phonon scattering induced by increasing temperature or alloying smears and weakens the lattice potential which in turn leads to a more "*s*" like Fermi surface.

Further, the ^{113}Cd Knight shift is found to be a useful tool for monitoring the phase segregation that occurs in Cd-Mg due to internal oxidation and for determining the concentrations of solutes such as Hg and Mg in Cd-Hg and Cd-Mg alloys.

Key words: Anisotropic Knight shift; Cd; Cd-Hg; internal Mg oxidation; isotropic Knight shift; Knight shift.

1. Introduction

The purpose of this paper is threefold: (1) To review the current theoretical and experimental situation with respect to Knight shifts and electronic structure in metallic Cd. The mechanisms which are thought to be responsible for the peculiar temperature dependences of the pure Cd Knight shift and bulk susceptibility are noted. The implications with respect to the Cd band structure of recent measurements of the Cd Knight shifts in Cd-Mg and Cd-Hg alloys are discussed. (2) To contribute some new experimental Knight shift data on solid solutions of isovalent Cd-Mg and Cd-Hg alloys. These include isotropic and anisotropic Knight shifts at ^{113}Cd and ^{199}Hg sites in Cd-Mg and Cd-Hg alloys. (3) To discuss the use of nuclear magnetic resonance as a sensitive probe of the kinetics of Mg oxidation which takes place in Cd-Mg alloys, and the use of the Knight shift to measure the alloy concentration.

2. General Observations

The isotropic and anisotropic Knight shift and the susceptibility of Cd are very temperature dependent. Earlier it was suggested that there might be a correlation between the temperature dependences of the Knight shift and the susceptibility [1].[1] Although a correlation between the isotropic and anisotropic Knight shift on the one hand and the susceptibility on the other exists, it is not linear as we will show below.

The isotropic part of the Knight shift of *hcp* Cd changes from 0.35 percent to 0.58 percent (an increase of 70%), in going from liquid helium temperatures to 594 K [1–5]. It further increases by 33 percent (to 0.79%) upon melting of the metal [2]. Over the same temperature range, the anisotropic part of the Knight shift varies by a factor of 6 in magnitude, and changes sign, progressing from −0.01 percent at liquid helium temperature [4–7] to 0.05 percent at [3, 8, 9] 300 K.

The magnetic susceptibility of pure Cd is diamagnetic and anisotropic [10]. There is a temperature dependence which is a function of the angle between the applied magnetic field (used in measuring the susceptibility) and the hexagonal symmetry axis (*c* axis). This is illustrated in figure 1. The susceptibility measured along the *c* axis, $\chi_{||}$, increases in magnitude by a factor of 3 in going from high to low temperature. The susceptibility measured perpendicular to the *c* axis $\chi_{\perp}$ is essentially temperature independent.

* Guest-worker at the NBS. Permanent address: Physical Technical Institute of Low Temperature (Academy of Sciences of the Ukr. SSR) Kharkov, 310086 USSR.

[1] Figures in brackets indicate the literature references at the end of this paper.

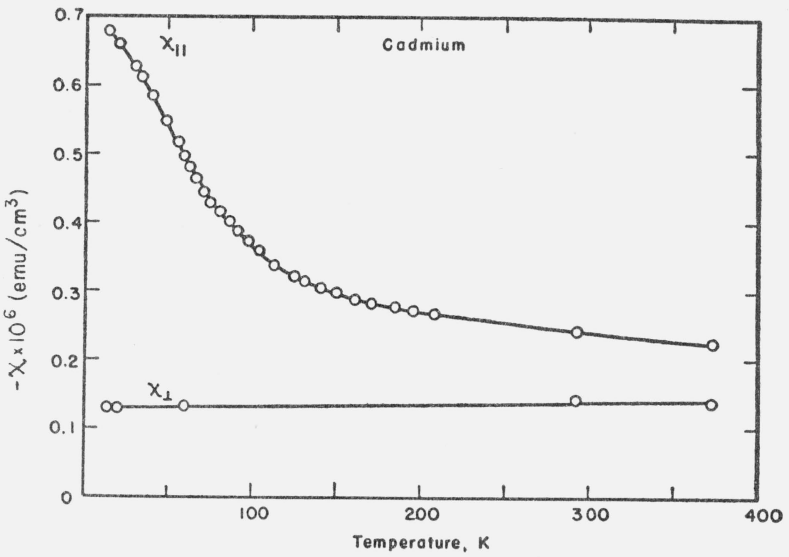

FIGURE 1. *The experimentally measured magnetic susceptibility of* Cd *metal single crystal as a function of temperature.*

$\chi_{\parallel}$ is the susceptibility measured parallel to the c axis and $\chi_{\perp}$ is the susceptibility measured perpendicular to the c axis. Both $\chi_{\parallel}$ and $\chi_{\perp}$ are diamagnetic. (From ref. [10]).

It is of interest to see whether or not the Knight shift and the susceptibility have the same functional dependence upon temperature, and thus a linear relationship to each other. Figure 2a shows the anisotropic Knight shift parameter $\mathcal{K}_{ax}$ as a function of the magnetic anisotropy, $\chi_{\parallel}-\chi_{\perp}$ and of the average susceptibility [11], $(\chi_{\parallel}+2\chi_{\perp})=3$ with temperature as the implicit variable. Figure 2b shows the isotropic Knight shift plotted against the average susceptibility. The data were obtained from the works previously mentioned [3, 4, 10]. The reason for plotting $\mathcal{K}_{ax}$ against $\chi_{\parallel}-\chi_{\perp}$ is to test for the possibility of a common orbital contribution [11]. The obvious departure from linearity in each case suggests that the Knight shift and susceptibility arise predominantly from different mechanisms. Temperature dependent terms other than spin paramagnetism must be operative in either the Knight shift or the susceptibility or both. This will be mentioned further in the following discussion.

The Brillouin zone and some parts of the Cd Fermi surface are shown [12] in figure 3. For our purposes the most important parts of the Fermi surface are the neck (waist) of the second zone hole monster (which appears in fig. 3a near point M), the third zone lens of electrons centered at point Γ, and the third zone needles of electrons at point K. Figure 3b shows a section in the plane MΓK using the repeating zone representation of the Fermi surface. The sections of the monster which are thought to contribute to the Knight shift are clearly visible in the figure.

The peculiar dependence of both isotropic and anisotropic shifts has been attributed to the effects of lattice vibrations on the Cd band structure [13, 14]. In the pseudopotential approximation, the increasing phonon modulation of the band structure weakens the pseudopotential [15] of pure Cd, leading to a more free electron like behavior at the Fermi surface. The important parts of the Fermi surface insofar as the Knight shift is concerned are the sections of 2d-zone-hole monster in the ΓM direction and lens of the third band, which are a mixture of "*s*" and "*p*" like electronic states [14]. At $T=0$ K, "*p*" contributions to the anisotropic Knight shift from the monster almost completely cancel the corresponding contribution from the lens. As the temperature is raised the decrease and symmetrizing of the pseudopotential increases the relative amount of "*s*" character on the monster at the expense of "*p*" character. However the electronic character at the lens is unaffected. It then follows that the isotropic and anisotropic Knight shifts will increase. The isotropic shift increases because of the corresponding increase in "*s*" character, the anisotropic shift because of the decrease in "*p*" character that opposes the positive lens contribution. The jump in isotropic shift at the melting point can be explained as an abrupt change in the density of states in the liquid state of the metal brought about by the disappearance of long-range order in the solid state [14, 16]. Calculations by Jena et al. [17] show that core polarization contributions do not exceed 10 percent of the low temperature isotropic Knight shift.

Kasowski [14] and Jena and Halder [16] have calculated the value of the Knight shift at selected temperatures between 0 K and the melting point and upon melting. On the basis of these theoretical works it is possible to partition the contributions to the changes in the isotropic Knight shift over three temperature ranges as shown in table 1. The table shows an oscillation in the importance of the roles played by the density

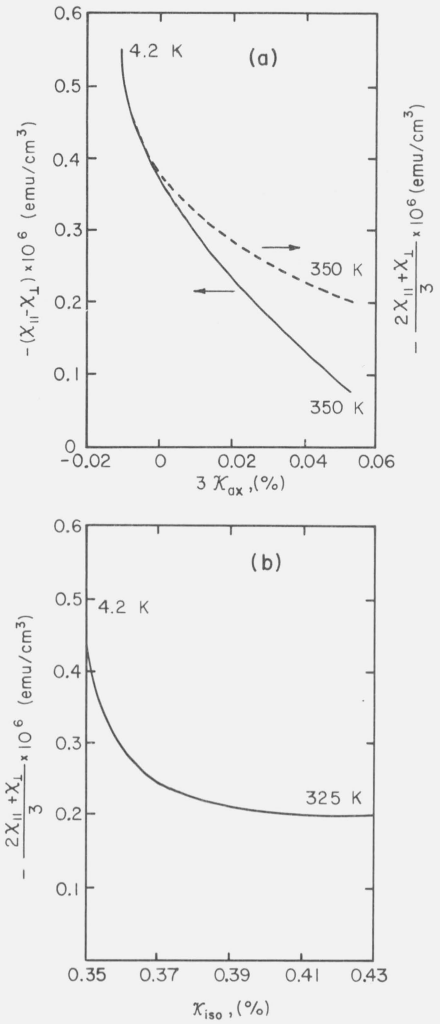

FIGURE 2. *Knight shifts of* ^{113}Cd *versus susceptibility with temperature as the implicit variable in the approximate range of 4.2 to 325–350 K.*

See text for definition of $\chi_{\parallel}$ and $\chi_{\perp}$.

(a) The anisotropic Knight shift is plotted against the experimentally measured magnetic anisotropy, $\chi_{\parallel}-\chi_{\perp}$, which is shown in solid curve. The anisotropic shift is also plotted against the averaged experimental susceptibility $(\chi_{\parallel}+2\chi_{\perp})/3$ which is shown as a dashed curve. Note that $\chi_{\parallel}-\chi_{\perp}$ is plotted on the left hand ordinate axis whereas $(\chi_{\parallel}+2\chi_{\perp})/3$ is plotted on the right hand ordinate axis.

(b) Isotropic Knight shift plotted against the averaged experimentally measured susceptibility. The data have been taken from refs. [3, 4, and 10].

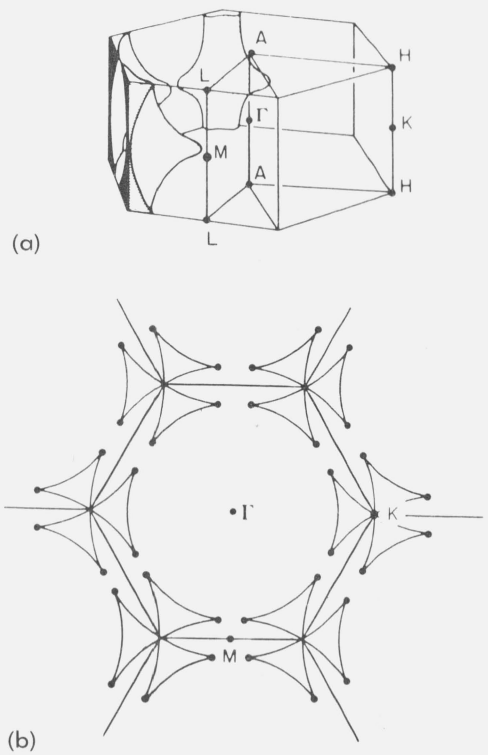

FIGURE 3. *Parts of the Fermi surface of* hcp Cd (*from ref.* [12]).

[a] Symmetry points of the Brillouin zone and second zone hole sheets in single-zone segments.

[b] Section in the MΓK plane (see text).

TABLE 1. *Partitioning of isotropic Knight shift changes between the density of states and the electronic density*

	Solid Cd			Liquid Cd
	0 K	462	594 [a]	
$\mathcal{K}_{iso}$,%)	0.35	0.47	0.59	0.79
$\Delta\mathcal{K}_{iso}$(%)	0.12	0.11	0.21	
% increase in $\mathcal{K}_{iso}$	34	24	36	
Fraction of $\Delta\mathcal{K}_{iso}$ due to density of states changes	1/2	1/8	4/5	
Fraction of $\Delta\mathcal{K}_{iso}$ due to explicit changes in $\langle\lvert\psi(0)\rvert^2\rangle_F$	1/2	7/8	1/5	

[a] Melting point.

of states and the wavefunction through the electronic density, $<|\psi(0)|^2>_F$, in producing the increases in isotropic shift observed in the solid at 462 and 594 K (the melting point) and in the liquid. Below 462 K the density of states accounts for half the change in Knight shift. Between 462 and 594 K the wavefunction structure presumably determined by the symmetrizing of the pseudopotential produces 7/8 of the increment observed in the measurement of $\mathcal{K}_{iso}$, the isotropic shift. It should be noted that in the region 0–462 K the density of states is found to increase by only 17 percent and thus the spin susceptibility increases from [14] 0.54 to 0.63×10^{-6} emu/cm^3. This would seem to rule out the possibility that the decrease in diamagnetic susceptibility might arise from an increase in spin paramagnetism.

In summarizing the situation for pure Cd,

(1) Neither the isotropic nor the anisotropic Knight shift is linearly proportional to the susceptibility.

(2) According to the recent work by Kasowski [14], most of the Knight shift (anisotropic and isotropic) temperature dependence can be explained by the changes in electronic character at the monster and

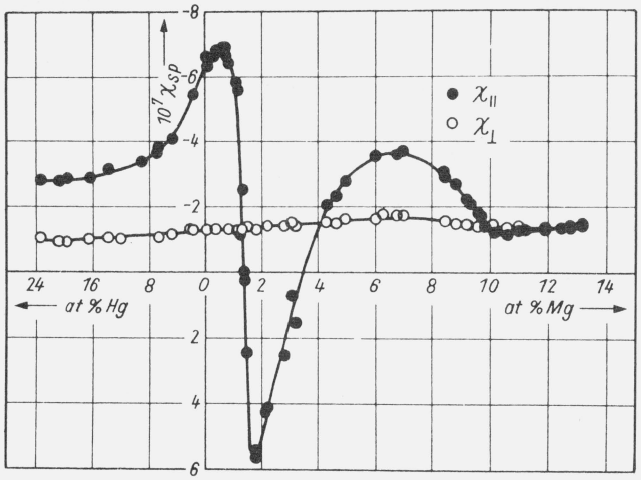

FIGURE 4 *Magnetic susceptibility of single crystal* Cd *alloys as a function of concentration of* Hg *and of* Mg *at 4.2 K.*

χ is plotted in emu/(cm)^3. The vertical scale is inverted so that χ values above the horizontal axis in the figure are diamagnetic. (From refs. [18 and 19]).

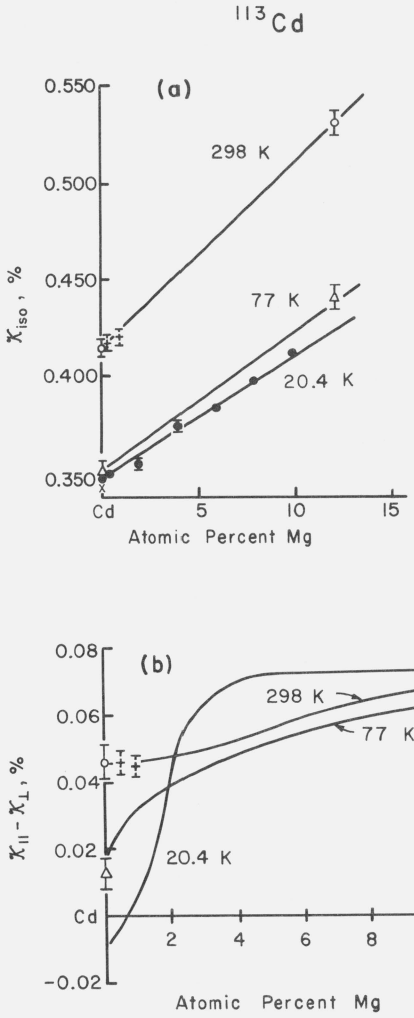

FIGURE 5. *Knight shifts at the* ^{113}Cd *site in* Cd-Mg *alloys as a function of* Mg *concentration at three different temperatures.*

(a) Isotropic shifts. The solid curves represent the data of Zhukov and Svechkarev (refs. [7, 20, 21]) at the indicated temperature. Some representative data points from their work are shown by the closed circles. The crosses are room temperature data points from Borsa and Barnes (ref. [3]), the x is from Williams and Sharma (ref. [4], and the open circles and triangles show data we have obtained in this investigation at respectively room and liquid nitrogen temperatures (assuming a nominal concentration of 12 at. % Mg). All data points have been scaled so that the pure ^{113}Cd Knight shift is 0.415 percent at 293 K. (ref. [30]). (b) Anisotropic shifts: The identification of the data is the same as in (a).

lens portions of the Fermi surface. This mechanism contributes only a small part of the change observed in the susceptibility.

In order to understand the electronic behavior in pure Cd a series of low temperature susceptibility measurements on Cd-Mg and Cd-Hg alloys were carried out by Svechkarev et al. [18, 19]. Their data, taken at 4.2 K, is shown in figure 4. The striking features in the variation of the susceptibility measured parallel to the *c* axis are the diamagnetic peaks at 0.5 and 6.5 at. % Mg and the sharp paramagnetic peak at 1.8 at. % Mg. Later Zhukov and Svechkarev [7, 20, 21] followed up with Knight shift measurements on the ^{113}Cd site in these alloys. They found that although the isotropic and anisotropic shifts increased with the addition of Mg or Hg neither one followed the drastic variations in the susceptibility reported by Svechkarev et al. [18, 19]. The data of Zhukov and Svechkarev along with that of others is shown in figures 5 and 6. In the interest of clarity their data points are shown only on the isotropic shift of Cd in Cd-Mg alloys at 20.4 K. McClure and Martyniuk [22] have calculated the orbital susceptibility of Cd as a function of Hg or Mg concentration under the assumption [18, 19] that the susceptibility behavior is dominated by contributions from electrons in closely spaced energy bands near Brillouin zone boundaries. Such a region occurs in the vicinity of symmetry point K in Cd. Their particular model calculation reproduces the experimental susceptibility behavior rather well.

It would then appear that the bulk susceptibility and iso- and anisotropic Knight shifts do not track one another with concentration because they are determined by distinctly different regions of the Fermi surface. In pure Cd, the Knight shift is primarily associated with the spin paramagnetism and wavefunctions on the parts of the Fermi surface in the vicinity of symmetry points M (monster) and Γ (lens) [14]. The principal contributions to the susceptibility come from the needles of the Fermi surface (point K). The variation in susceptibility as a function of Mg and Hg alloying arises from a turning off and on of an orbital (diamagnetic term) rather than a large increase in spin paramagnetism. The potential changes introduced by alloying with isoelectronic Mg and Hg produce an approximately monotonic variation in the isotropic and anisotropic Knight shifts which are quite different than the drastic changes in the diamagnetic susceptibility introduced by interband electronic contributions at point K [18, 19]. This would explain why no corresponding drastic changes in the Knight shift are observed. Such a finding is also consistent

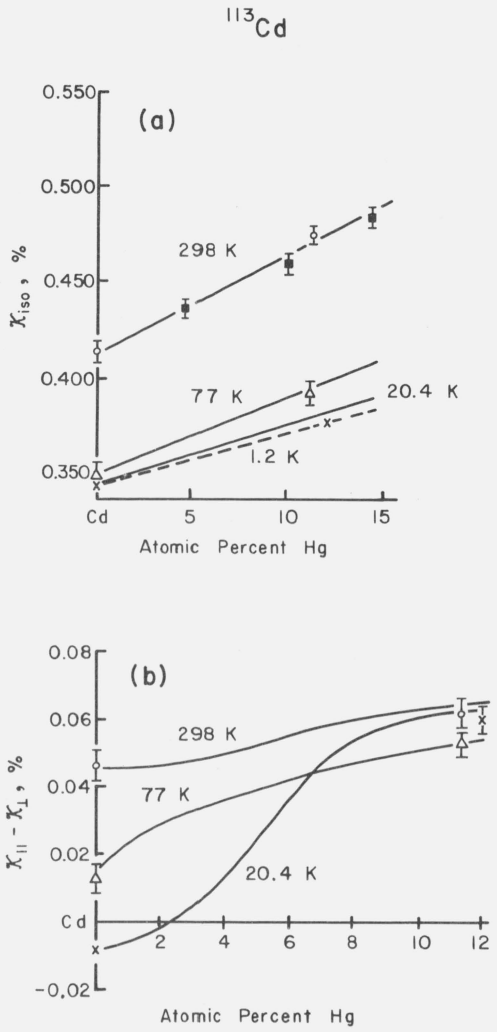

FIGURE 6. *Knight shifts at the* ^{113}Cd *site in* Cd-Hg *alloys as a function of* Hg *concentration between liquid helium and room temperatures.*

(a) Isotropic shift: The solid curves represent the data of Zhukov and Svechkarev at 20.4, 77 and 298 K (refs. [7, 20, 21, and 25]). The open circles and triangles reflect new data from this study at respectively room and liquid nitrogen temperatures. The x's are superimposed from the 1.2 K data of Williams and Sharma (ref. [4]) and the closed squares are from the work of Grant and Henry at room temperature (ref. [34]). All data points have been scaled so that the pure ^{113}Cd Knight shift is 0.415 percent at 298 K and 0.350 percent at 4.2 K. (ref. [30]).

(b) Anisotropic shifts: The identification of data is the same as in (a). The datum from Williams and Sharma (ref. [4]) for Cd+12 at. % Hg was plotted under the assumption that these authors give $\frac{1}{3}(\mathcal{K}_{||} - \mathcal{K}_{\perp})$. (From ref. [35]).

with recent Knight shift measurements [23] on Ga, Al, and In in pseudobinary alloys of $AuGa_2$, $AuAl_2$, and $AuIn_2$ and with Knight shift and susceptibility measurements on ^{71}Ga in $AuGa_2$ at temperatures above 500 K [24]. In the case of $AuGa_2$ at high temperatures it is found that the susceptibility is increasing, with increasing temperature while the Knight shift is relatively constant.

In addition Zhukov and Svechkarev [17, 21, 25] have experimentally extracted the concentration dependence of the structure of the wavefunctions insofar as they contribute to the ratio $3\mathcal{K}_{ax}/\mathcal{K}_{iso}$. Figure 7 is a plot of this ratio as a function of concentration for Cd-Mg and Cd-Hg at 20.4 K and as a function of temperature for pure Cd. The three curves are similar in form and suggest a correlation between impurity concentration and temperature in terms of affecting the wavefunction (band structure) via the lattice potential. Figure 8 expresses this correlation directly where the temperature calibration has been provided by the pure Cd in figure 7.

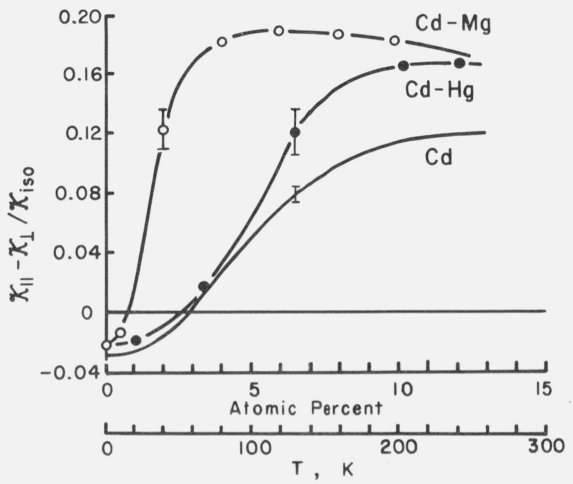

FIGURE 7. *Ratio of* ^{113}Cd $(\mathcal{K}_{||} - \mathcal{K}_{\perp})/\mathcal{K}_{iso}$ *plotted against concentration (in at. %) of* Mg *and* Hg *in* Cd-Mg *and* Cd-Hg *alloys respectively at 20.4 K and against temperature in pure* Cd.

A typical error bar is indicated on each curve. (From refs. [20 and 21]).

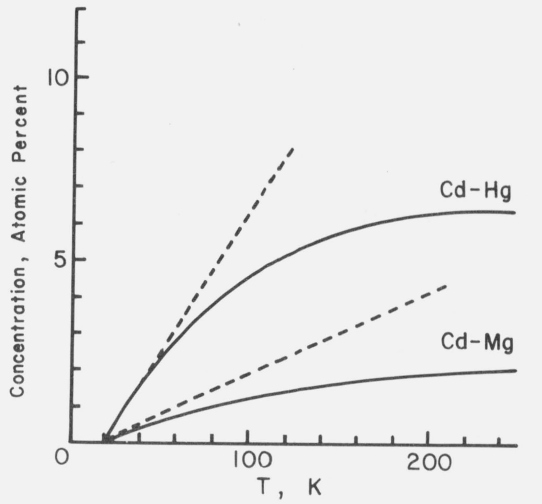

FIGURE 8. *Concentration-temperature correspondence based on the* ^{113}Cd *ratio* $\mathcal{K}_{ax}/\mathcal{K}_{iso}$ *extracted from figure 7 for* Cd-Mg *and* Cd-Hg *alloys.*

See text. The dotted lines are the slopes of the curves at C = 0. Note that in the case of Cd-Mg it takes 3–4 times less solute than in Cd-Hg to produce an effect on the lattice potential equivalent to the same change in temperature. (From refs. [20 and 21]).

3. New Experimental Data

3.1. Sample Preparation, Characterization and Experimental Procedure

The Cd-Mg alloy was prepared by melting weighed amounts of the constituents under flux in a resistance furnace. The molten alloy was mixed by stirring with a graphite rod and then chill cast in a steel mold. The powder was obtained by remelting the ingot in a 350 °C paraffin oil bath contained in a stainless steel beaker. A high speed homogenizer (7000 rpm) operating under the bath comminuted the alloy. After cooling to 70 °C the particles and oil were sieved with a 200 mesh screen. After further cooling to room temperature the paraffin was removed using hexane in a dry box. The dried powder was sieved and the 325 mesh particles were sealed in a glass capsule at 10^{-5} torr and annealed at 300 °C for 100 h. After resieving through a 325 mesh screen the passed particles were found to be spheres of average diameter 10 μm.

According to the phase diagram (fig. 9) the alloy prepared, Cd + 12 at.% Mg, is probably in the solid solution range. Oxidation [27] of the Mg was a problem here and will be discussed in detail in the next section. Weighed amounts of Cd and Hg were allowed to react with each other at room temperature for about 12 h in order to reduce the vapor pressure and minimize the hazard of heating liquid Hg. The Cd-Hg alloys were then prepared by melting the constituents in a quartz tube sealed under 10^{-5} torr vacuum. A resistance furnace which maintained a temperature of 400 °C was used for the melt. Mixing was assured by shaking the molten metal several times. The alloy was then cast by inverting the quartz tube allowing the molten material to freeze in a cool extension of the quartz tube. After cooling the ingot was transferred to a glass tube sealed under 10^{-5} torr vacuum and homogenized for 100 h at 250 °C.

The powder was prepared by filing the ingot under liquid nitrogen using a number 4 cut file, and collecting only those particles which would pass through a 325 mesh screen. These filings were sealed under 10^{-5} torr vacuum in a glass tube and annealed 6 h at 250 °C. Sieving through a 325 mesh screen was then repeated. According to recent Cd-Hg phase diagram measurements by Claeson et al. [28], our Cd-Hg alloys lie within the α-phase solid solution range (fig. 10). The filings were found to be small irregular foils with an average thickness of 10 μm.

The Cd-Mg alloy powder prepared under oil was examined by x-ray diffraction. Interpolation between the measured lattice parameters and the diagram of Svechkarev and Solnyshkin [27] indicated that the sample contained 9.4(1) at. % Mg. Two weeks after preparation, additional x-ray lines attributable to "pure" Cd metal were seen. The intensities of the Cd lines were approximately equal to those of the alloy lines. Three weeks later the powder was reexamined with the x-ray diffractometer and broadening as well as substantial weakening of the alloy lines were noted along with strong sharp lines for metallic Cd. The growth of the Cd x-ray lines with time is associated with internal oxidation discussed in section 3.4. The discrepancy in the composition between the x-ray

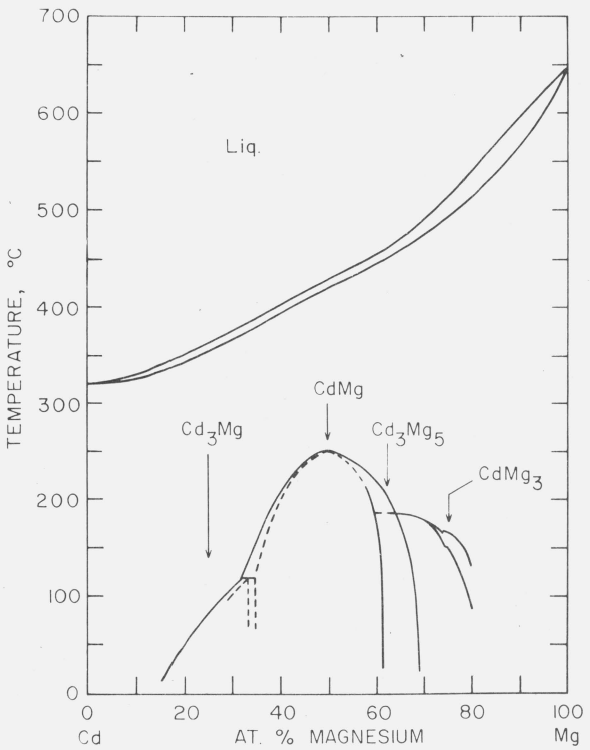

FIGURE 9. Cd-Mg *phase diagram.*

The Cd + 12 at. % Mg alloy is probably within the α-phase solid solution region (From ref. [26]).

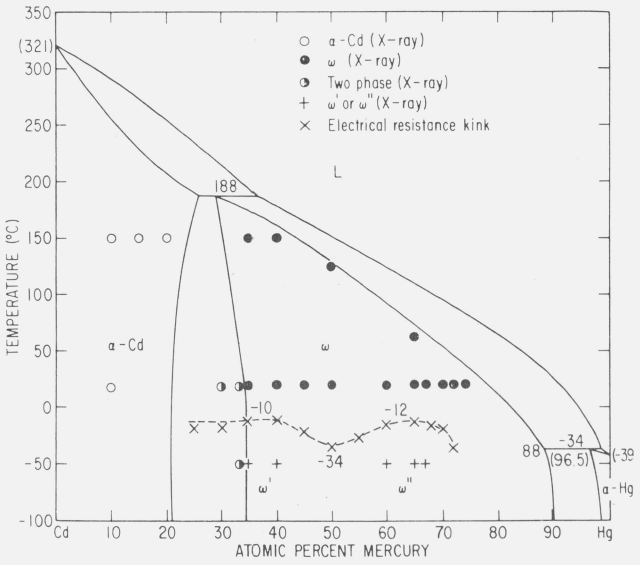

FIGURE 10. Cd-Mg *phase diagram.*

An alloy of Cd + 12 at. % Hg is well within the α-phase solid solution region. (From ref. [28]).

measurement and the weighed (12 at. % Mg) constitutents is not understood at the present time but we will consider that the alloy concentration is about 12 at. % because this is the nominal composition and because this value agrees with the NMR data shown in figure 5a. It would be useful to use other analytical techniques, including perhaps electron microprobe, to resolve this matter. Simultaneous with the x-ray determinations, NMR measurements were made on this alloy with the interesting result that the Knight shift may be more precise than the x-ray diffraction pattern for obtaining the concentration in the presence of phase segregation.

X-ray diffraction patterns on the Cd-Hg alloys yielded the Hg concentrations shown in table 2. The interpolation between concentration of Hg and lattice parameter is also taken from the work of Svechkarev and Solnyshkin [27].

Measurements of the Knight shift were made on a Varian[2] wide line crossed coil spectrometer (V-4200B) at magnetic fields of 16kG(^{113}Cd) and 10kG(^{199}Hg). A signal averaging computer (Varian C-1024) was employed with repetitive field sweeps to improve signal to noise. To obtain temperatures of 4.2 and 77 K, a cold finger Dewar was inserted into the probe. For studies at these temperatures the sample was sealed in a glass vial under a fraction of an atmosphere of helium gas.

The resonance parameters were measured using the ^{113}Cd and ^{199}Hg isotopes both of which have spin $I=1/2$ and thus the spectra are not complicated by quadrupole effects. The skin depth at these frequencies exceeds the average particle dimensions in the pure Cd at 77 K and in the Cd alloys at all temperatures. The isotropic and anisotropic Knight shift parameters were extracted using the method of Lebedev [7, 29].

TABLE 2. *Concentration of* Hg (*at. %*) *in* Cd-Hg *alloys determined by x-ray diffraction and NMR*

Nominal concentration[a]	X-ray diffraction determination	Isotropic Knight shift determination
1.5		1.6(5)
3		2.4(5)
6	5.6(5)	6.0(5)
8	8.1(3)	8.2(5)
10	9.3(3)	9.6(5)
12	11.3(3)	12.0(5)

[a] As determined by initial weighing of constituents prior to alloy preparation.

3.2. Knight Shift Results

Some NMR line profiles on pure Cd were made at 16kG at room and at nitrogen temperatures in this study in order to improve the accuracy of the lower field anisotropy measurements of the previous study [7, 21, 25]. An illustration of the resolution of the ^{113}Cd powder pattern available at the higher fields at $T=298$ K is shown in figure 11.

The Cd NMR in a Cd+12 at. % Hg alloy was investigated. The numbers obtained for the isotropic and anisotropic Knight shifts on the ^{113}Cd site at two temperatures (77 K and 298 K) agree reasonably well with data from the previous work (see figure 6).

The ^{199}Hg resonance was observed in all of the Cd-Hg alloys – described in section 3.1. The isotropic and anisotropic Knight shifts which were measured at 4.2, 77 and 298 K are plotted against concentration in figure 12. The concentrations were determined from the ^{113}Cd Knight shifts as will be described in the section on metallurgical applications. The linewidths with the anisotropy subtracted out [7, 29] varied between 15 and 20 G. The more dilute alloys had the narrow lines. Knight shifts of the ^{199}Hg in the alloy were referenced to ^{199}Hg in liquid Hg metal at room temperature. The Knight shift of ^{199}Hg was taken as 2.72(1) percent [30].

By combining the isotropic Knight shift data from the previous work with the numbers from this study (fig. 5 and fig. 6) it is possible to obtain a linear least squares fit to the isotropic shift versus concentration, C, in the case of **Cd**-Mg, **Cd**-Hg and Cd-**Hg**. The equations of the line of $\mathcal{K}$ (C) versus C at 4 temperatures are listed in table 3. In the case of **Cd**-Hg at 4.2 K only two points from Williams and Sharma [4] were used to obtain the slope of the line. Note that the slope of $\mathcal{K}$ (C) provides a practical method of measuring C to within $\pm 1/2$ at. %.

3.3. Discussion of Knight Shift Results

It should be noted that the behavior of both isotropic and anisotropic ^{199}Hg shifts as a function of alloying was qualitatively similar to the corresponding curves at the ^{113}Cd site (fig. 6). This would confirm that the Cd and Hg atom are observing a common band structure. Similar behavior in which solvent and solute atom "see" a common band structure has been found pre-

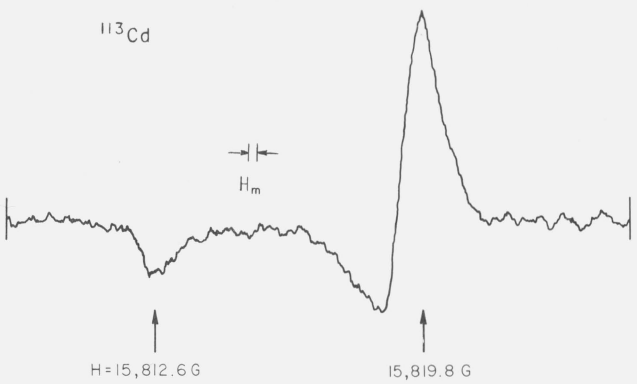

FIGURE 11. *Typical trace of the* ^{113}Cd *absorption derivative spectrum versus magnetic field in pure metallic* Cd *powder at 298 K and at 16kG.*

A modulation of 0.25G and an integrator time constant of 0.3 s were employed. The trace represents 250 digitally stored sweeps each of 25 s duration through the line.

[2] This instrument is identified in order to adequately specify the experimental procedure. In no case does such identification imply recommendation or endorsement by the National Bureau of Standards, nor does it imply that the instrument identified is necessarily the best available for the purpose.

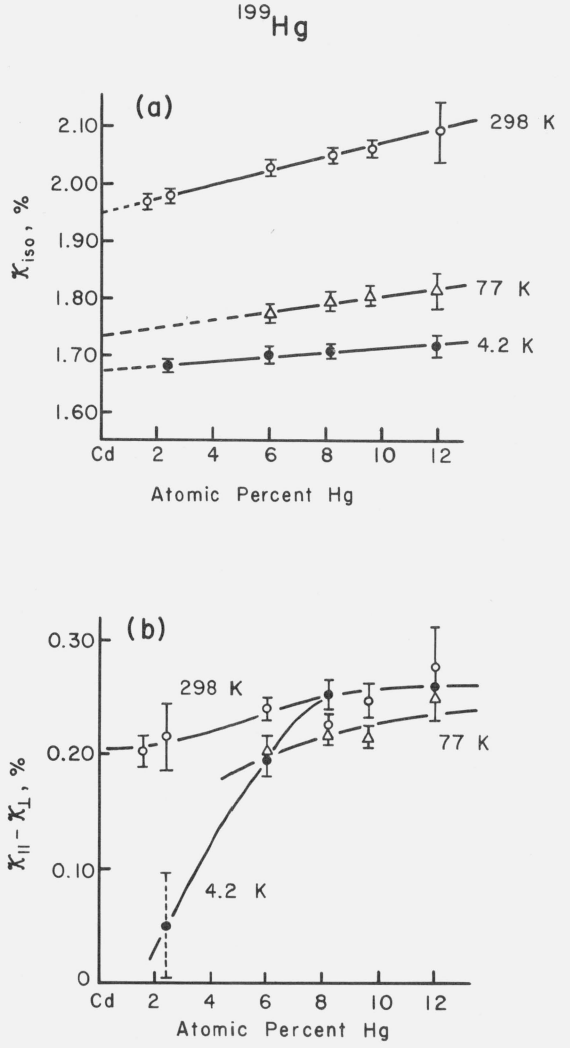

FIGURE 12. *Knight shifts of* ^{199}Hg *in* Cd-Hg *alloys versus* Hg *concentration.*

The open circles are 298 K data, the triangles are 77 K data and the closed circles are 4.2 K data.

(a) Isotropic Knight shifts. The solid lines represent least squares fits to the data and the dashed lines are extrapolations of the fitted lines to C=0.

(b) Anisotropic Knight shift. The large uncertainty (dashed bar in the 4.2 K datum) was introduced by the combined effects of low Hg concentration and noise from random sample motion in the liquid helium bath.

TABLE 3. *Isotropic Knight shifts (in %) as a function of solute* (Mg *or* Hg) *concentration,* C, *(in at. %) from least-squares fits to the data in figures 5a, 6a and 10a*

$$\mathcal{K}(C) = \mathcal{K}_0 + \Delta\mathcal{K} \cdot C$$

Temperature K	Cd-Mg (^{113}Cd site)		Cd-Hg (^{113}Cd site)		Cd-Hg (^{199}Hg site)	
	$\mathcal{K}_0$	$\Delta\mathcal{K}$	$\mathcal{K}_0$	$\Delta\mathcal{K}$	$\mathcal{K}_0$	$\Delta\mathcal{K}$
4.2			[a] 0.350 + 0.0025C		1.674 + 0.004C	
20.4	0.350 + 0.006C		0.350 + 0.003C			
77	0.353 + 0.007C		0.353 + 0.004C		1.737 + 0.007C	
298	0.415 + 0.009C		0.415 + 0.005C		1.952 + 0.012C	

[a] This value of $\mathcal{K}_{iso}$ was obtained only from two points (see text).

viously in pseudobinary alloys [23] of $AuGa_2$ and $AuIn_2$.

We have evaluated the ratio $[\mathcal{K}_{Hg}(C)/\mathcal{K}_{Cd}(C)]$ in the Cd-Hg alloys at C=0, 5, 10 at. % Hg and at 4.2, 77 and 298 K. The values for the three concentrations were averaged together at each temperature and the results are shown in table 4. The average over all 3 temperatures is listed at the bottom of the table. In the simplest possible common band picture, this ratio should be equal to the ratio of hyperfine fields in the free atoms [9], $H_{Hg}^{atom}/H_{Cd}^{atom} = 3.69$. This follows because

$$\mathcal{K} \propto \xi H^{atom} \chi_p$$

in which ξ is the fractional amount of electronic "*s*" character at the site and χ_p is the spin susceptibility.

The deviation of the experimental ratio $[\mathcal{K}_{Hg}/\mathcal{K}_{Cd}]$ from the theoretical estimate of $H_{Hg}^{atom}/H_{Cd}^{atom}$ may imply unequal ξ factors at the two sites. For example if it is assumed that $\xi_{Cd} = 0.33$ in Cd metal [9] the ξ_{Hg} has a value of 0.42 in the Cd alloy. This is to be compared [9] with $\xi_{Hg} = 0.21$ in solid metallic Hg. Interestingly enough, $\xi_{Hg} = 0.49$ in the liquid [30].

To ascertain the effects of volume changes on the ratio $\mathcal{K}_{Hg}/\mathcal{K}_{Cd}$, we list in table 5 the atomic sizes of Mg, Cd, and Hg evaluated using four different criteria [31]. It is clear from table 5 that in all cases the atomic size increases in going from Cd to Hg. The Cd lattice compresses the Hg solute relative to a metallic Hg lattice and if other factors are ignored, the product ξH_{Hg} would be larger than in solid Hg metal. However the decrease in size using any of the criteria in table 5 lead to volume changes that are too small to explain the observed factor of two increase in ξ.

TABLE 4. *Average ratio of* ^{199}Hg *and* ^{113}Cd *Knight shifts*

Temperature, K	$[\mathcal{K}_{Hg}/\mathcal{K}_{Cd}]$
4.2	4.68(9)
77	4.77(14)
298	4.58(10)
Total average:	4.67(11)

TABLE 5. *Atomic sizes of* Mg, Cd *and* Hg *(from Pearson ref.* [31])

	Pearson's atomic volume (Å)^3	Pauling's single bond radii valence 2 (Å)	Pauling's ionic radii valence 2 (Å)	Teatum, Gschneider and Waber CN 12 radii (Å)
Mg	23.240	1.364	0.65	1.602
Cd	21.581	1.485	0.97	1.568
Hg	23.4	1.490	1.10	1.573

Figure 13 shows the increased ξ factor of Hg as a probe in Cd superposed on the ξ factors computed for a large number of pure metals. The new point, i.e., ^{199}Hg in Cd (closed circle) appears more appropriate to the Ag-Cd-In row than the ^{113}Cd in Cd. A possible explanation is that the Cd lattice already has an anomalously low ξ_{Cd} factor [9] because of anisotropy effects. Adding Hg destroys the anisotropy by producing a dis-

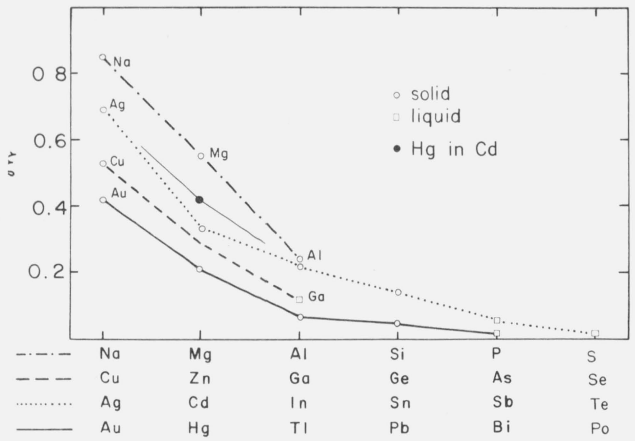

FIGURE 13. *Behavior of ξ factors for metallic elements as a function of their position in the periodic table.*

(From ref. [9]). The ^{199}Hg site ξ factor (0.42) obtained in Cd-Hg alloys is shown as a closed circle. This point is related to Ag on one side and to In on the other by the partially extended solid line. The ξ value is to be contrasted with the ξ factor of ^{113}Cd (0.33) in Cd. See text.

ordered lattice with weaker and a more symmetric lattice potential [14, 20, 21]. This in turn leads to an increase in electronic "*s*" character at the Fermi surface which is sensed by both the ^{113}Cd and ^{199}Hg Knight shifts.

3.4. Metallurgical Applications of the Knight Shift

Using the x-ray measurement of concentration, the isotropic and anisotropic Knight shifts for one alloy, Cd + 12 at. % Hg, are shown at 77 and 298 K in figure 6. The room temperature point fits reasonably well on the straight line constructed from previous data where the concentrations were deduced from more extensive x-ray diffractometry. Alternatively, it was possible to assign Hg concentrations in Cd-Hg alloys by measuring the room temperature isotropic ^{113}Cd Knight shift and superimposing this value on the curve corresponding to 298 K in figure 6a. Both the x-ray and Knight shift determinations of the Hg concentration in these alloys are shown in table 2. It should be noted that the concentrations determined from the Knight shifts are in good agreement with the x-ray determinations in four alloys. The ^{113}Cd lineshapes indicated that the alloys were all single phase.

Another application was the use of the ^{113}Cd isotropic Knight shift to study the kinetics of Mg oxidation in the Cd-Mg alloy. We found that the isotropic Knight shift provides a more precise method for monitoring the kinetics of Mg oxidation mentioned earlier in connection with sample preparation than conventional x-ray diffractometry. This is illustrated in figure 14 where four traces of the Cd spectrum from the Cd + 12 at. % Mg alloy taken during a 2 month period at room temperature are shown in chronological order. Approximately 2 weeks after sample preparation, oxidation of the Mg and its effective removal from the solid solution matrix is evident by the appearance of the pure Cd line on the right-hand side of the figure. On the

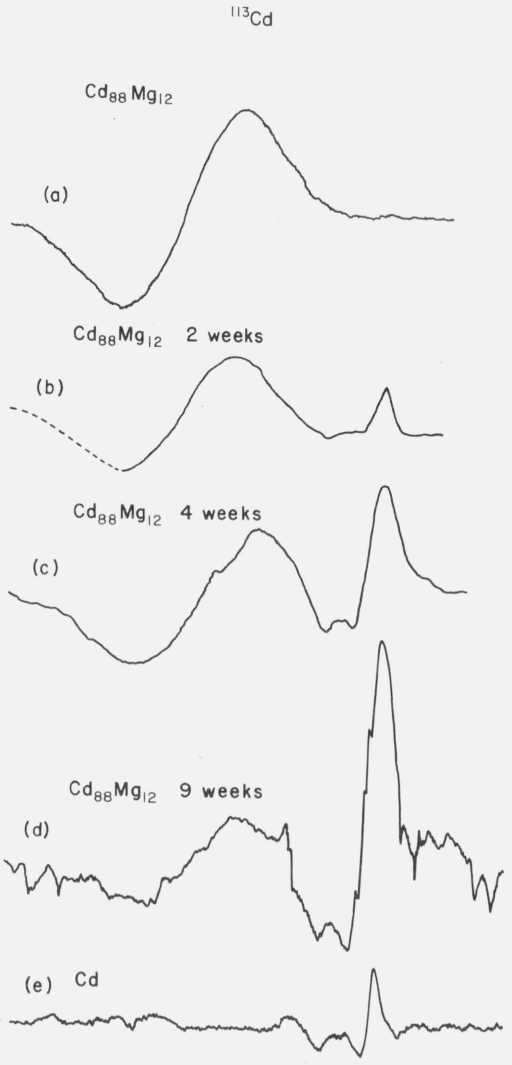

FIGURE 14. *Traces of the ^{113}Cd absorption derivative spectrum in an alloy (initially prepared to be a* Cd + 12 *at. %* Mg *alloy) versus magnetic field (increasing to the right) at room temperature in the neighborhood of 16kG. In each case the narrow line on the right corresponds to "pure" metallic* Cd *and the broader line on the left corresponds to the alloy.*

(a) Spectrum observed immediately after sample was prepared. There is no trace of "pure" Cd.
(b) Spectrum observed two weeks after sample was prepared, with the sample stored at room temperature in a screw-cap vial. The relative NMR intensity of "pure" Cd is 5 percent.
(c) Spectrum observed 5 weeks after sample was prepared. The relative NMR intensity of "pure" Cd is 16 percent.
(d) Spectrum observed 9 weeks after sample was prepared. The relative NMR intensity of "pure" Cd is 54 percent.
(e) Spectrum of ^{113}Cd in a sample consisting only of pure metallic Cd under the same experimental conditions as (a) through (d).

basis of figure 5a it is possible to assign a concentration of 12.5(5) at. % Mg to the shifted alloy line visible on the left-hand side of figure 11b. The relative amount of "pure" metallic Cd in the alloy phase is about 5 percent as determined from the resonance intensity of the spectrum [32]. At this point the x-ray diffraction indicated the existence of a pure Cd line but the intensity was insufficient to permit its resolution from

the main alloy line. When the trace in figure 11c was taken the relative intensity of "pure" Cd had increased to 16 percent with no change in the isotropic shift of the alloy. An x-ray measurement at approximately the same time that this trace was made, indicated a two-phase region with well resolved alloy and "pure" Cd peaks. In figure 11d the "pure" Cd NMR intensity is approximately 54 percent of the total. Again the isotropic shift of the alloy phase is unchanged. The investigation of Svechkarev and Solnyshkin [27] showed that the Mg oxidation proceeds to a depth of 20 μm below the surface of a solid Cd-Mg alloy after which no further Mg precipitation occurs. Since the bulk of the alloy in our sample is in the form of spheres of 10 μm diam, the oxidation process would ultimately remove all the Mg from the solid solution leaving only "pure" Cd and probably an oxygen-magnesium complex. Presumably the x-rays see only the atoms approximately 1 μm and less below the surface. On the contrary the NMR sees the entire particle to the extent that the rf skin depth exceeds the diameter. Furthermore because the Knight shifts of the two metallic phases are distinct, the NMR is capable of monitoring the intensity ratios throughout the interval over which the Mg is being oxidized. In addition the NMR observations suggest that the kinetics of this process are such that the Mg is continuously removed from the metallic phase at progressively increasing depths below the surface. There do not appear to be any intermediate Cd phases in this process, otherwise a third Cd Knight shift would be expected. It is important to mention that here is another system in which the NMR can be an important metallurgical monitoring probe in studying kinetics [32–33].

4. Conclusion

The ^{113}Cd and ^{199}Hg isotropic and anisotropic Knight shifts have been measured in Cd-Mg and Cd-Hg alloys. The ^{113}Cd shifts are in agreement with previous work. The ^{199}Hg shifts in Cd-Hg qualitatively reproduce the behavior of the ^{113}Cd shifts in the same alloys as a function of Hg concentration. However the ratio of ^{199}Hg to ^{113}Cd isotropic shift exceeds the corresponding hyperfine field ratio suggesting that the relative fraction of electronic "*s*" character at the Fermi surface is greater in the alloy than in either of the pure metals. Volume changes are too small to account directly for the observed increase in the ^{199}Hg ξ factor. The increase in "*s*" character at the Hg site is consistent with the theoretical model of the anisotropic Cd band structure in which phonon scattering induced by increases in temperature or alloying leads to a weaker more symmetric lattice potential.

Recent nonlocal pseudopotential band calculations [36] on Cd-Mg and Cd-Hg alloys tend to support this approach. These calculations are for the most part in agreement with the results of the earlier simpler local potential approach [20, 21]. For example, in Cd-Mg it is found that changes in the Knight shift can probably be related to the variation in the energy spectrum produced by decreases in lattice constant and c/a induced by alloying with Mg. On the other hand in Cd-Hg it is probably necessary to take into account the impurity scattering which produces an effect similar to the Debye-Waller factor [14] (phonon scattering) in order to explain the Knight shifts.

The recent band calculation also shows that the energy spectrum at the needles (point K) is insensitive to Debye-Waller modulation of the lattice potential. This provides a justification for the explanation of the variations in susceptibility [18, 19] in which smearing of the lattice potential has been neglected [22].

An interesting metallurgical observation is that the ^{113}Cd Knight shift is a useful probe for studying phase segregation and for measuring solute concentrations in Cd-Hg alloys.

We are indebted to D. B. Fickle for sample preparation, to R. L. Parke for technical assistance and to C. J. Bechtoldt for the x-ray diffractometry measurements. We thank R. E. Watson, H. Schone, J. Gardner, P. Soven, J. R. Anderson, and R. V. Kasowski for helpful discussions. We also acknowledge the assistance of G. C. Carter and D. J. Kahan of the Alloy Data Center, NBS.

5. References

[1] Schone, H. E., Phys. Rev. Letters **13,** 12 (1964).
[2] Seymour, E. F. W., and Styles, G. A., Phys. Letters **10,** 269 (1964).
[3] Borsa, F., and Barnes, R. G., J. Phys. Chem. Solids **27,** 567 (1966).
[4] Williams, D., and Sharma, S. N., Can. J. Phys. **48,** 1416 (1970).
[5] Goodrich, R. G., Khan, S. A., and Reynolds, J. M., Phys. Rev. **3B,** 2379 (1971).
[6] Sharma, S. N., and Williams, D. L., Phys. Letters **25A,** 738 (1967).
[7] Zhukov, V. V., Zhuk, G. M., Svechkarev, I. V., Phys. Nizk. Temp. N17, 3, FTINT AN Ukr. SSR, Kharkov (1972) (In Russian).
[8] Drain, L. E., Metal. Rev. **119,** 195 (1967).
[9] Bennett, L. H., Watson, R. E., and Carter, G. C., J. Res. Nat. Bur. Stand. (U.S.), **74A** (Phys. and Chem.), No. 4, 569–610 (July–Aug. 1970).
[10] Marcus, J., Phys. Rev. **76,** 621 (1949).
[11] Ross, J. W., Fradin, F. Y., Isaacs, L. I., and Lam, D. J., Phys. Rev. **183,** 645 (1969).
[12] Hurd, C. M., The Hall Effect in Metals and Alloys (Plenum Press, New York, 1972).
[13] Kasowski, R. V., and Falicov, L. M., Phys. Rev. Letters **22,** 1001 (1969).
[14] Kasowski, R. V., Phys. Rev. **187,** 891 (1969).
[15] Stark, R. W., and Falicov, L. M., Phys. Rev. Letters **19,** 795 (1967).
[16] Jena, P., and Halder, N. C., Phys. Rev. Letters **26,** 1024 (1971).
[17] Jena, P., Das, T. P., Gaspari, G. D., and Mahanti, S. D., Phys. Rev. **1B,** 1160 (1970).
[18] Svechkarev, I. V., and Kusmicheva, L. B., Phys. Status Solidi, Sol. **37,** K113 (1970).
[19] Svechkarev, I. V., Kusmicheva, L. B., and Poltoratsky, V. I., Magnetic Properties of Zinc and α-phase of Binary Solid Solutions of Mercury and Magnesium in Cadmium, FTINT AN Ukr. SSR, Kharkov (1972) (In Russina).

[20] Zhukov, V. V., Zhuk, G. M., and Svechkarev, I. V., Abstracts of Reports at the XVIIth Congress Ampere, Turku, Finland (Aug. 1972). Full text in English available from authors upon request.
[21] Svechkarev, I. V., Zhukov, V. V., and Zhuk, G. M., Phys. Nizk. Temp. N20, 77, FTINT AN Ukr. SSR, Kharkov (1972) (In Russian).
[22] McClure, J. W., and Martyniuk, J., Phys. Rev. Letters **29,** 1095 (1972).
[23] Carter, G. C., Weisman, I. D., Bennett, L. H., and Watson, R. E., Phys. Rev. **B5,** 3621 (1972).
[24] Warren, W. W., Jr., Shaw, R. W., Jr., Menth, A., DiSalvo, F. J., Storm, A. R. and Wernick, J. H., Phys. Rev. **B7,** 1247 (1973).
[25] Zhukov, V. V., Fenster, M. Ia., Svechkarev, I. V., and Zhuk, G. M., Phys. Nizk. Temp. N18, 58, FTINT AN Ukr. SSR. Kharkov (1972) (In Russian).
[26] Phase diagram prepared by the National Bureau of Standards Alloy Data Center from Hansen, M., Constitution of Binary Alloys (McGraw-Hill Book Co., Inc., New York 1958) and Elliott, R. P., Constitution of Binary Alloys, First Supplement (McGraw-Hill Book Co., Inc., New York, 1965).
[27] Svechkarev, I. V., and Solnyshkin, D. D., Phys. Nizk. Temp. N18, 119, FTINT AN Ukr. SSR, Kharkov (1972) (In Russian).
[28] Claeson, T., Luo, H. L. Anantharaman, T. R. and Marriam, M. F., Acta Met. **14,**285 (1966).
[29] Lebedev, Ya. S., J. Struct. Chem. 4, 19 (1963) (Translated from: Zhurnal Structurn. Khimii **4,** 22 (1963)).
[30] This value is the result of a critical evaluation of Knight shifts by the National Bureau of Standards Alloy Data Center.
[31] Pearson, W. B., The Crystal Chemistry and Physics of Metals and Alloys (Wiley Interscience, New York, 1972).
[32] Bennett, L. H. and Carter, G. C., Met. Trans. **2,**3079 (1971).
[33] Bennett, L. H., Acta Met. **14,**997 (1966).
[34] Grant, R. F., and Henry, W. G., Can. J. Phys. **39,** 841 (1961).
[35] Daughterty, M., and Hewitt, R. R., Phys. Rev. **5B,** 3450 (1972).
[36] Kasowski, R. V., private communication.

(Paper 77A6–794)

520-812 O-LF - 73 - 3